Appendix I

DEVELOPMENT OF THE LARMOR CONDITION[1]

Let S′ be a frame of reference rotating with respect to the laboratory frame S with an angular velocity represented by the vector $\vec{\omega}$.

According to the general law of relative motion, the time derivative $\dfrac{d\,\vec{A}}{d\,t}$ of any time dependent vector $\vec{A}(t)$ computed in the laboratory frame S, and its derivative $\dfrac{\delta\,\vec{A}}{\delta\,t}$ computed in the moving frame S′ are related through[2]

$$\frac{d\,\vec{A}}{d\,t} = \frac{\delta\,\vec{A}}{\delta\,t} + \vec{\omega} \times \vec{A} \tag{I1}$$

In particular if we consider the vector angular momentum $\vec{I}$, then by replacing $\vec{A}$ by $\vec{I}$ in equation (I1) we have

$$\frac{d\,\vec{I}}{dt} = \frac{\delta\,\vec{I}}{\delta\,t} + \vec{\omega} \times \vec{I} \tag{I2}$$

which rearranges to

$$\frac{\delta\,\vec{I}}{\delta\,t} = \frac{d\,\vec{I}}{d\,t} + \vec{I} \times \vec{\omega} \tag{I3}$$

An expression for $\dfrac{d\,\vec{I}}{d\,t}$ is now determined. From elementary electromagnetic theory the torque $\vec{\tau}$ on a magnetic moment in a magnetic field $\vec{B}_o$ is given by

$$\tau = \vec{\mu} \times \vec{B}_o \tag{I4}$$

Since

$$\vec{\tau} = \frac{d\,\vec{I}}{d\,t} \tag{I5}$$

then

$$\frac{d\,\vec{I}}{d\,t} = \vec{\mu} \times \vec{B}_o \tag{I6}$$

and substituting for $\vec{\mu}$ using equation (1) this gives

$$\frac{d\,\vec{I}}{d\,t} = \gamma\,\vec{I} \times \vec{B}_o \tag{I7}$$

Substituting equation (I7) into equation (I3) gives

---

[1]We follow here the development of Abragam p19.

[2]For a proof of equation (I1) see for example Symon p 271.

I-1

$$\frac{\delta \vec{I}}{\delta t} = \gamma \, \vec{I} \times \vec{B}_o + \vec{I} \times \vec{\omega} \tag{I8}$$

or

$$\frac{\delta \vec{I}}{\delta t} = \gamma \, \vec{I} \times \left(\vec{B}_o + \frac{\vec{\omega}}{\gamma} \right) \tag{I9}$$

By comparing (I9) to (I7) it follows that in the rotating frame, the effective field which is seen is

$$\vec{B}_e = \vec{B}_o + \frac{\vec{\omega}}{\gamma} \tag{I10}$$

If the rotating frame has an angular velocity such that

$$\vec{B}_o = -\frac{\vec{\omega}}{\gamma} \tag{I11}$$

then the effective field in the rotating frame is zero. Also $\dfrac{\delta \vec{I}}{\delta t} = 0$ and so $\vec{I}$ is a fixed vector in the rotating system. This means that in the laboratory frame, $\vec{I}$ precesses about $\vec{B}_o$ with a frequency

$$\vec{\omega}_L = -\gamma \, \vec{B}_o \tag{I12}$$

where $\left| \omega_L \right|$ is called the LARMOR FREQUENCY.

In summary, in a magnetic field, the angular momentum $\vec{I}$ and the magnetic moment $\vec{\mu}$ precess at the Larmor frequency given by equation (I12), and when a frame of reference is rotating at the Larmor frequency the magnetic field (which gave rise to the precession at the Larmor frequency) is zero in the rotating reference frame.

Appendix II
EFFECT OF ROTATING FIELDS ON TRANSITIONS

We will continue to use the notation of Appendix I so that $\vec{B}_o$ is the static field in S. The linearly polarized field $\vec{B}_1$ in S gives rise to a constant field $\vec{B}_1$ along the x axis in S′ and it rotates with S′ about $\hat{k}$ (or $\vec{B}_o$) in S at a rate ω.

The total field $\vec{B}_e$, which is shown in figure II1, is static in S′ and is given by

$$\vec{B}_e = \left(B_o + \frac{\omega}{\gamma} \right) \hat{k} + B_1 \hat{i}. \tag{II1}$$

The unit vectors $\hat{i}$ and $\hat{k}$ are in S, and the $\hat{k}$ component is zero for the Larmor frequency as was shown in Appendix I.
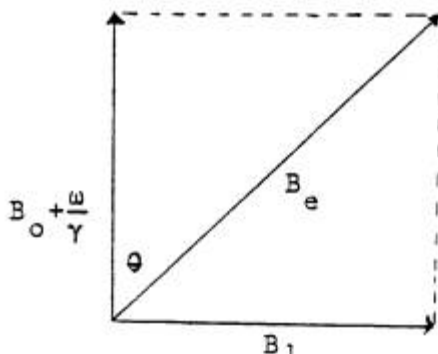

Figure II1: Effective Field in the Rotating Frame of Reference.

The angle θ between $\vec{B}_e$ and $\vec{B}_o$ is given by

$$\tan\theta = \frac{B_1}{B_o + \dfrac{\omega}{\gamma}} = \frac{-\gamma\,B_1}{-\gamma\,B_o - \omega} \tag{II2}$$

where ω is the rate of precession of $\vec{B}_1$ about $\vec{B}_o$. Using equation (I12) and the analog for ω_1

$$\omega_1 = -\gamma B_1 \tag{II3}$$

equation (II2) becomes

$$\tan\theta = \frac{\omega_1}{\omega_L - \omega} \tag{II4}$$

From this equaiton θ is never large or the effect of B_1 is negligible unless $\omega \approx \omega_L$ or $\omega_L - \omega \approx \omega_1$. The width of the resonance, that is, the value of the difference $|\omega - \omega_L|$ below which the effect is appreciable is of the order of ω_1. You should be able to show that $\vec{B}_1$ is of the order of 15 gauss and hence you can calculate the magnitude of ω_1 as a fraction of ω_L for this experiment.

If a linearly polarized field is composed of two components, one rotating with angular frequency of ω, then the other has an angular frequency of $-\omega$. At resonance, for one component $\omega = \omega_L$ and for the second $\omega = -\omega_L$. For the second component

$$\tan\theta = \frac{\omega_1}{2\,\omega_L} \tag{II 5}$$

and hence $\theta \approx 0$ because $\omega_1 \ll \omega_L$. Thus absorption of power is due only to the component where $\omega = \omega_L$.

Appendix III

GaAs GUNN DIODES

The discovery that microwaves could be generated by applying a steady voltage across a crystal of gallium arsenide was made in 1963 by J.B. Gunn. The Gunn diode is not a diode in the sense that it is junction since it is bulk property device but only in the sense that it is a two port device. The brief description of Gunn diodes given here can be supplemented with material from books like Bulman, Hobson, Shurmer or Streetman.

The Gunn Effect Mechanism

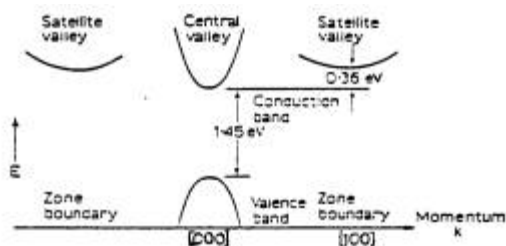The band structure for GaAs is given in figure III-1.

Figure III-1: Band Structure for GaAs.

The mechanism responsible for the Gunn effect, sometimes called the "transferred electron mechanism", is that of transfer of electrons from the lowest valley in the conduction band to valleys of higher energy where the mobility is less, leading to negative differential resistivity and travelling domains of high electric field within the semiconductor.

The first effect of applying an increasing electric field across a specimen of gallium arsenide is to increase the energy and momentum of electrons in the central valley. When the field is high enough for electrons to gain an energy of 0.36 eV they may remain in the central valley, but most of them will transfer to a satellite valley in which the density of states is high and the effective mass of the electron is very large. The associated momentum change is produced by longitudinal optical phonons. As a result, the electron mobility falls by a factor of 50 times, and this accounts for the region of negative differential conductivity indicated in figure III-2.

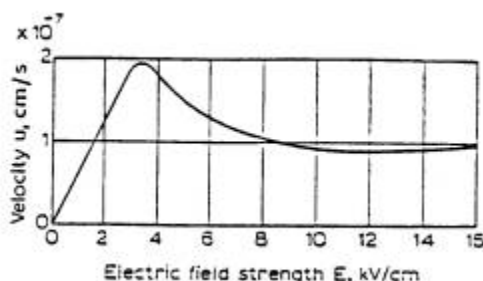

Figure III-2: Average Electron Velocity vs Field Strength for GaAs.

The threshold for negative differential conductivity varies with material and is typically 3000 V/cm for GaAs. If the GaAs is biased so that the field falls in the negative conductivity region, then if there is an increase in electric field due to a random fluctuation of charge as the current is drifting, the mobility of the

electrons will decrease in the region of the increased field. Electrons ahead will move away and electrons behind will pile up. This space charge fluctuation which usually forms near the cathode and builds up exponentially is called a Gunn domain. The drifting domain reaches the anode where it gives up its energy as a pulse of current.

Modes of Operation of Gunn Diodes

The Gunn diode can be operated in a number of different modes. The simple drift of stable domains or **transit time mode** results in a current waveform composed of a series of spikes which appear with a frequency equal to the inverse transit time, v_s/L. This mode, although easy to understand and usually the first to be discussed in texts is not appropriate for efficient conversion of D.C. to microwave power because of the narrowness of the current pulses. It is also not useful for applications requiring frequency control of the Gunn oscillator since the frequency is determined by the transit time of the domains.

There are several modes of operation in which the transit time of space charge and domains through the device is **not** the frequency control. Frequency control is obtained by placing the Gunn diode in an external high Q resonant cavity such as that shown in figure III-3 so that the circuit reacts on the Gunn effect device and impresses a sinusoidal voltage waveform on the D.C. bias as is shown in figure III-4. We shall discuss the most important modes, the delayed domain mode, the quenched domain mode, the limited space charge accumulation (LSA) mode and the hybrid mode.

For the **delayed domain mode**, the Q factor of the resonant circuit and the impedance Z_L of the load must be large enough so that the sinusoidal
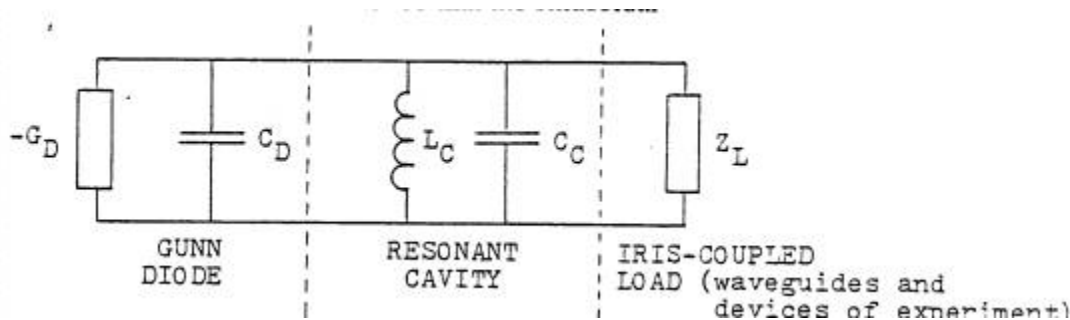
-G_D = negative conductance of the Gunn diode
C_D = parasitic capicitance of the Gunn diode
L_C = inductance of the resonant cavity
C_C = capacitance of the resonant cavity
Z_L = load impedance

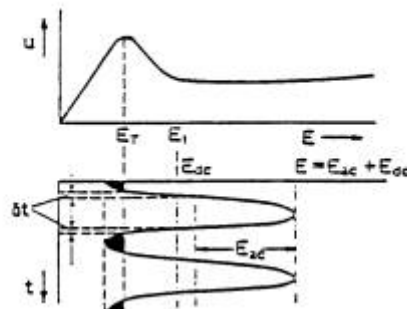Figure III-3: Equivalent Circuit of a Gunn Oscillator.

Figure III-4: A.C. Voltage Impressed on the D.C. Bias of a Gunn Diode.

voltage waveform amplitude at the device terminals is large enough to cause the voltage to fall below threshold E_T over a portion of each cycle. The domain transit time must be less than the resonant period of the circuit so that the domain may disappear into the anode while the voltage is below threshold. The next domain is not nucleated until the voltage once more rises above threshold. The formation of domains is thus controlled by the resonant period of the circuit and this is the big advantage of this mode over the transit time mode.

In the **quenched domain mode**, the impedance Z_L is still larger and the alternating field created within the specimen by the external circuit will be large enough to drive the net field below a minimum sustaining value while the domain is in transit and thus cause the domain to be extinguished. The next domain will be nucleated when the terminal voltage again rises through threshold. The difference between this mode and the delayed domain mode is that in the quenched domain mode, frequencies higher than the transit time frequency can be generated.

In any mode where domains are formed there will be very high electric fields in the region of the domain. This can cause impact ionization and breakdown and result in destruction of the device. To prevent this, only small voltages may be applied across the device and this will result in low power output. Also, in modes where the transit time is important for frequency control, the physical size of the device must be kept small and this too will limit output power of the device.

In the **limited space charge accumulation (LSA) mode** one does not allow domains to form and so higher terminal voltages (giving higher rf power output) may be applied to the device without causing impact ionization. Also, the device length is not related to the frequency and may be many times the distance electrons would drift during one period at the operating frequency. In these devices which are sometimes called overlength devices, the output power depends directly on the material volume.

Domains do not form instantaneously but in a time called the dielectric relaxation time which depends on the differential mobility of the electrons. In order that domains do not form, the time δt which is spent during one oscillation in the region between E_T and E_1 in figure III-4 must be small compared with the average negative dielectric relaxation time between E_T and E_1. As the electric field rises above threshold and into the region between E_T and E_1, space charge inhomogeneities begin to form. Before they have grown to a significant size, the electric field must become large enough for the instantaneous negative differential mobility to fall to a very low value. Thus, space charge perturbation can be limited to a very small value if the dielectric relaxation time, averaged over the time that electric field exceeds threshold, is greater than the rf period. Also, the time spent below threshold during each cycle (shaded areas) must be long enough for dissipation of the space charge growth which occurs when the voltage swings above threshold. Another way of saying this is to say that in order to avoid successive build up of small amounts of space charge over many cycles, it is necessary for the positive differential mobility damping to exceed the negative differential mobility growth.

Although LSA devices have high output power they are difficult to fabricate. The doping of the sample and the design of the frequency controlling cavity are critical if the conditions mentioned in the paragraph above are to be met. In addition, the internal homogeneity of the low field conductivity must be better than about 10 per cent to avoid internal injection of significant dipolar space charge.

Hybrid mode devices, which are similar to LSA mode devices have less strigent conditions to fulfill and are easier to fabricate. When doping is not uniform enough for LSA operation the space charge growth during one cycle, when terminal voltage exceeds threshold, is sufficient for dipolar domains to form incipiently. The growth does not proceed to the quasi-static domain equilibrium inherent in the quenched domain mode, and operation has partly an LSA and partly a quenched domain character. As the terminal

voltage falls below threshold, dipolar space charge begins to dissipate but it is not completely quenched before the voltage again rises through threshold. Accordingly, it again grows into an incipient domain during the next cycle of operation. If the device is sufficiently long, it will contain multiple domains, each of the same size but separated spatially by the transit distance per cycle. The dipolar space charge is eventually quenched as it enters the anode. The presence of the domains causes the current to be less than it would be in the LSA operation and thus the efficiency of hybrid operation is less than that of LSA operation but greater than that of quenched mode devices. The presence of multiple domains in the hybrid device means that the peak electric field is less than in a quenched domain device where there is a single domain. Thus the likelihood of avalance breakdown is less, or alternatively the device can be operated at higher bias voltages to generate more power.

Fabrication and Device Construction

The active region of the Gunn diode where there is negative resistance and in which domains may form is composed of n-active GaAs in which the dopant is commonly Sn, Se or Te. Diodes can be made from slices of a bulk single crystal from a melt but all useful devices are made from epitaxial GaAs. Epitaxy or epitaxial growth is the technique of growing an oriented single crystal layer on a single crystal substrate. Liquid phase epitaxy, vapour phase epitaxy and molecular beam epitaxy are various techniques of epitaxial growth.

A typical epitaxial Gunn diode structure is shown in figure III-5. The starting point is a heavily doped substrate of bulk grown single crystal GaAs to define the single crystal growth and to give mechanical strength to the thin active region of the device. When designating relative doping
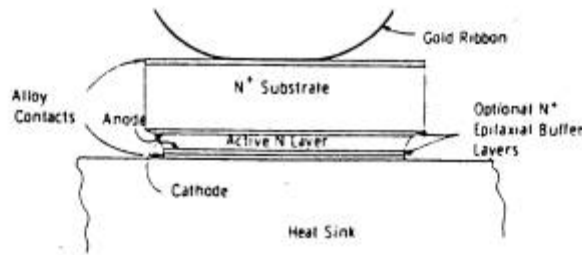

Figure III-5: Typical Epitaxial Gunn Diode Structure.

concentrations on diagrams of devices such as in figure III-5, it is common to use + and - symbols. Thus a heavily doped (low resistivity) n-type layer would be referred to as n^+ material. It has become common practice to grow an epitaxial "buffer" layer of highly doped n^+ material on the highly doped substrate in order to reduce propagation of crystal defects and diffusion of impurities from the substrate into the active region of the device. Metallic contacts are often made onto low resistivity n^+ epitaxial "buffer" layers.

The active region is epitaxially grown with the doping a couple of orders of magnitude less than in the substrate. Doping concentrations vary depending on the application but are typically 2×10^{15} cm^{-3} for X band microwave devices. The length of the active region is typically 10μm and one can see that the critcial field is reached for an applied voltage of 3 volts. The product of doping concentration, times the device length for this typical device is 2×10^{12} cm^{-2} and that value is typical of practical continuous wave devices. The mode of operation for these typical parameters is a mixture of several of the previous mentioned modes. The relative proportion of each mode depends quite sensitively on the bias voltage, the conductivity uniformity and the circuit loading.

The physical construction of the Gunn diode is shown in figure III-6. The overall geometry is

roughly 200 μm square with a length of 10μm. It is in a package of less than 1 mm^3 which is mounted on a 3-48 screw. The whole package is a couple of mm in diameter and less than a half a centimeter long. The mounting of the Gunn diode at the end of a post in the centre of the resonant cavity allows electric field oscillations within the Gunn diode to excite a particular TE resonant mode in the cavity. The most likely resonant mode can be deduced by the physical location of the post and Gunn diode. The diode waveguide circuit shown in figure III-6 does not show the varactor diode which is used for frequency tuning.
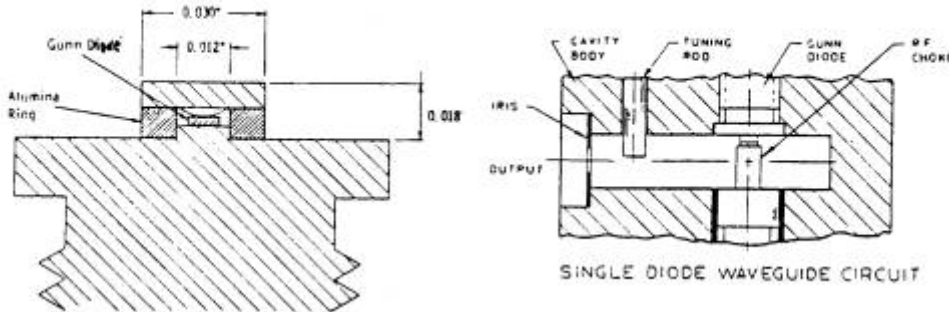
Figure III-6: Physical Construction of a Typical Gunn Diode.

Frequency Control With a Varactor Diode

     The resonant cavity capacitance, C_C, may be varied with a variable capacitance (varactor) diode to give frequency control over the microwave oscillations. The term varactor is a shortened from of variable reactor, referring to the voltage variable capacitance of a reverse biased p-n junction. The varactor diode is also made of properly doped GaAs and is fabricated from liquid phase, expitaxially grown p-n junctions much in the same way that the Gunn diode is made. The mechanical mounting and electrical connections are similar to that of the Gunn diode as well. As is shown in figure III-7,
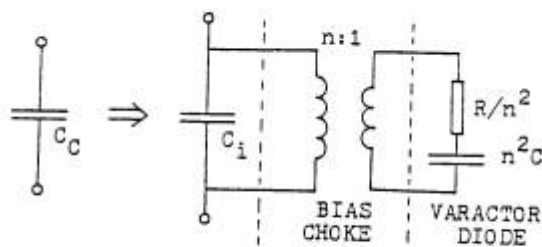
C_C = capacitance of the resonant cavity (total)
C_i = intrinsic capacitance of the cavity (i.e. air dielectric)

Figure III-7: Coupling of the Varactor Diode to the Cavity Capacitance.

the varactor diode is on the end of a bias choke (which isolates the rf and provides the D.C. bias) and it is inserted into the resonant cavity much as the quartz tube is inserted into the sample cavity in this experiment. The capacitance of the junction is of the order of 1 pF and it varies roughly as $V^{-1/2}$ where V is the D.C. bias. This means that the resonant frequency of the Gunn oscillations may be varied by varying the D.C. bias to the varactor diode.

The Varian VSX-9011-ND Gunn Effect Oscillator

A test performance sheet for the VSX-9011-ND is given in figure III-8. For a fixed operating voltage (bias voltage) the oscillator may be electrically tuned by varying the varactor voltage. The frequency increases by about 0.005 GHz per volt. A suitable operating bias voltage is 9.5 V. The frequency also depends on the bias voltage and will decrease if the bias voltage is lowered. All voltages should be applied slowly from zero. In the VSX-9011-ND there is a mechanical tuning rod but it should **never** be adjusted.

varian ·TEST PERFORMANCE SHEET

Type _VSX-9011-ND_ s/n _1491_
Date _9/15/91_ By _____

OCT 1, 1961

VARACTOR-TUNED GUNN EFFECT OSCILLATOR
OPERATING CHARACTERISTICS

MECH. FREQ. GHz	8.9	9.1	9.3					
VARACTOR FREQ. GHz		—						
OPERATING VOLTAGE Vdc		9.5						
OPERATING CURRENT Adc @ ___°C								
OPERATING CURRENT Adc @ +30°C		.590						
THRESHOLD CURRENT Adc @ ___°C								
THRESHOLD CURRENT Adc @ +30°C		.798						
* POWER OUTPUT MW @ ___°C								
* POWER OUTPUT MW @ +30°C	51	53	54	52	57	52		
* VARACTOR VOLTAGE Vdc @ ___°C								
* VARACTOR VOLTAGE Vdc @ +30°C	40	263	4.0	30.0	40	268		
ELECTRONIC TUNING MHz	0	+60	0	+60	0	+60		
POWER TEMP COEFF dB/°C		—						
FREQ. TEMP COEFF MHz/°C		—						

* LOAD VSWR ≤ 1.1:1 UNLESS OTHERWISE SPECIFIED.

† POLARITY INDICATED.

NOTES: 1. FOR BEST ELECTRONIC TUNING AND NOISE PERFORMANCE THE MINIMUM VARACTOR TUNING VOLTAGE SHOULD BE + ___4.0___ Vdc

2. FOR BEST ELECTRONIC TUNING AND NOISE PERFORMANCE THE MAXIMUM VARACTOR TUNING VOLTAGE SHOULD BE - ___40.0___ Vdc

Figure III-8: Test Performance Sheet for the VSX-9011-ND Oscillator.

Appendix IV
SPECIFICATIONS FOR THE MODEL X532B WAVEMETER

Model	G532A	J532A[1]	H532A	X532B
Frequency Range (GHz)	3.95-5.85	5.3-8.2	7.0-10	8.2-12.4
Overall Accuracy[2]	0.065%	0.065%	0.075%	0.08%
Calibration Increments	1 MHz	2 MHz	2 MHz	5 MHz
Scale Length in. (mm)	155 (3937)	140 (3556)	125 (3145)	77 (1956)
Dial Accuracy[3]	0.033%	0.033%	0.040%	0.050%
Fits Waveguide (in.) (EIA)	2 x 1 WR187	1-1/2 x 3/4 WR137	1-1/4 x 5/8 WR112	1 x 1/2 WR90
Equiv Flange	UG-407/U	UG-441/U	UG-138/U	UG-39/U
Max Temp Coef %/°C	0.0012	0.0012	0.0015	0.0010
Size, in., (mm) Length Height Depth	6-1/4 (159) 9-1/2 (241) 5 (127)	6-1/4 (159) 9-1/8 (232) 5-1/2 (114)	6-1/4 (159) 8 (203) 4-3/8 (111)	4-1/2 (114) 6-1/8 (156) 2-7/8 (73)
Net Weight lb, (kg)	9-1/2 (4, 1)	7-1/2 (3, 4)	6 (2, 7)	3-1/2 (1, 6)

FOR ALL MODELS

DIP AT RESONANCE: 1 dB or more
MINIMUM CALIBRATION SPACING: 1/32 inch

[2] Includes dial accuracy, 20°C temperature variation (23° ±10°C) and 0.02% for 0 to 100 relative humidity.

[3] Includes mechanical tolerances and backlash.

Appendix V
OPERATION OF THE BELL 620 GAUSSMETER
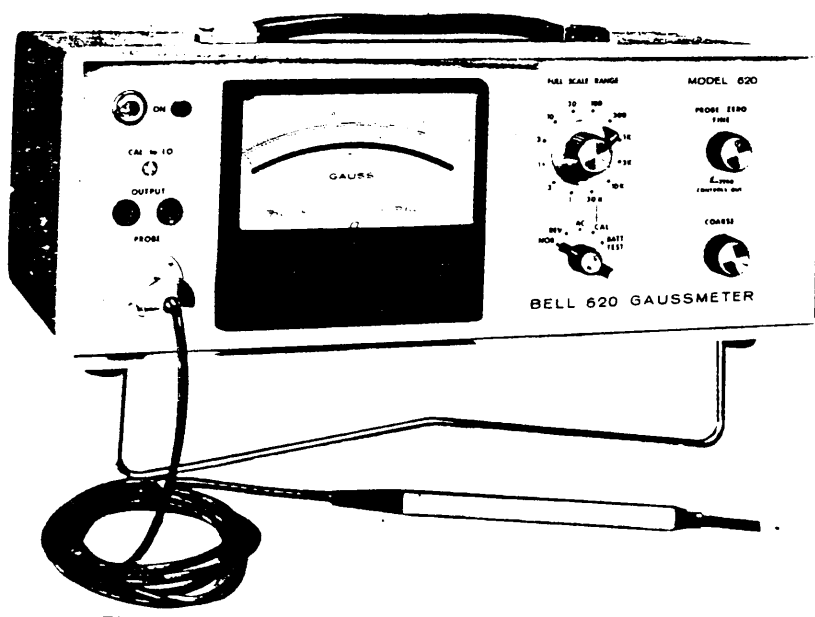
FRONT PANEL CONTROLS

Full Scale Range
Instrument covers the range from 0.1 gauss to 39K gauss.

Probe Zero (Fine and Coarse)
Zeroing controls to provide zero output in the absence of a magnetic field. See **Zeroing Procedure**.

    a.   NOR - normal position

    b.   REV - for measuring fields with reverse polarity

    c.   A.C. - for measuring A.C. fields

    d.   CAL - position for checking internal calibration. See **Calibration Procedure**.

    e.   BATT - battery test position if internal battery is used.

CAL TO 1.0
Potentiometer for calibration. See **Calibration Procedure**.

Output Jacks
- accepts standard banana plugs
- back jack is grounded to case

- red jack gives positive output voltage proportional to the full scale field for upscale readings (negative for below zero readings)
- output voltage 1.0 V D.C. full scale
- source impedance 1 KΩ
- main A.C. field frequency 400 Hz

Normal Operating Procedure

Turn the FULL SCALE RANGE switch to 30 K. Turn the function switch to NOR and turn on the power. Place the probe in the field to be measured and reduce the range until there is a meter indication. If the meter reads less than zero, turn the probe head through 180° or turn the function switch to REV

Zeroing Procedure

Insert the probe into the zero gauss chamber accessory (mu metal can). Rotate the RANGE switch counter clockwise until a reading is obtained on the meter. Adjust the ten turn COARSE control to bring the reading near zero while reducing the RANGE setting. Below the 1 gauss range, the FINE control may be used for better resolution of zero adjustment.

NOTE: Before removing the probe from the zero gauss chamber, turn the RANGE switch up to at least 1 to avoid off scale readings due to the earth's magnetic field.

Zeroing controls may also be used to suppress small residual fields up to approximately 30 gauss.

Calibration Procedure

Although the instrument is well calibrated, this adjustment should be made when very accurate readings are required.

After the instrument and probe have warmed up (5 min.), set the RANGE switch to the 30K range and the FUNCTION switch to CAL. Adjust the CAL screwdriver adjustment to obtain a full scale (1.0) meter reading, or, if a voltmeter is connected to the output jacks, a 1.0 V reading.

The internal calibration procedure is referenced to a standard NMR magnet traceable to the National Bureau of Standards.

Meter Tracking Error

For a D.C. field meter readout: ±1% of full scale.
For an A.C. field meter readout 10 to 400 Hz: ±2% of full scale.

Accuracy

The accuracy is limited by the sum of the internal calibration error, the linearity of the probe and meter scale errors for meter readout.

II-1 ELECTRICAL AND PERFORMANCE SPECIFICATIONS

(a) Measurement Ranges:

Measurement of static (dc) or varying (ac to 400 Hz) magnetic field strength in the range of 0.1 gauss full scale to 30.000 gauss full scale in 10 db steps as follows:

0.1	3	100	3,000
0.3	10	300	10,000
1.0	30	1,000	30,000

(b) Calibration:

1. Internal calibrating procedure is referenced to a standard NMR magnet traceable to the National Bureau of Standards and to probe deviation curves. Probe deviation curves in accordance with MIL-STD-793-1 (WP) Appendix A.

2. Internal calibration error does not exceed ±0.3%.

(c) Available Standard Probe Types:

One hundred and ten different Hall effect field probes are available to meet the challenging requirements of virtually any application. Please see the F.W. Bell Gaussmeter Probes literature sheet for probe models and prices. Consult the factory for special probe requirements.

(d) Accuracy:

1. Accuracy is the sum of the accuracies of the instrument, the probe and the calibration source. The instrument accuracy is ±0.25% of reading, and the internal calibration accuracy is ±0.3% of reading. For example, assume a 620 Gaussmeter used with a model STJ4-0404 probe calibrated with the internal calibration output. The total accuracy is ±0.25% (instrument), plus ±0.3% (internal calibration), plus ±0.1% (probe) for a total accuracy of ±0.65% of reading.

2. For ac Fields:
0 to 60 Hz: dc field accuracy
60 to 400 Hz: dc field accuracy plus ±10% of reading

3. Meter Scale Tracking Error:
For dc field meter readout; ±1% of full scale

For ac field meter readout 10 to 400 Hz; ±2% of full scale

II-2 PHYSICAL SPECIFICATIONS, CONTROLS AND CONNECTORS

(a) Front Panel:

1. Power Switch:
This toggle switch turns on the primary power to the instrument. The pilot indicates when the instrument is operating on line voltage only, no indication of battery operation is provided. See cautionary note in Section II-2b4.

2. Range Switch:
The full scale range is set by this switch in 10 db steps marked in the 1, 3, 10 sequence. It covers the range from 0.1 gauss to 30 k gauss, the full range of the instrument.

3. Function Switch:
This switch selects the mode of operation. It includes the measurement positions for dc fields of both normal and reverse polarities and for ac fields, the calibration position for internal CAL, and a battery test position

4. Improved accuracy obtainable by using probe deviation curves and, at specific test points, by reference to a known calibration field.

(e) Stability:

1. Line voltage:
Error unmeasurable for ±10% line voltage changes

2. Temperature effects excluding probe influences:
Approx. ±3% of reading total over the range of −50°C to +70°C (can be removed by using internal calibration feature).

3. Probe temperature effects, 1X sensitivity:
−0.04% of reading per degree C max.
−0.025% of reading per degree C typical. (−20°C +60°C)

4. Probe temperature effects, 10X sensitivity:
±0.005% of reading per deg. C mean value over −20°C to +60°C

5. Probe temperature effects, Zero Field Influence:
±100 milligauss per deg. C standard probes
±40 milligauss per deg. C high accuracy probe

(f) Output Jacks:

1. Output voltage:	1.0 volt dc FS
2. Source impedance:	1 kΩ approx.
3. Maximum ac field frequency:	400 Hz
4. Response time for full scale step input:	0.4 msec approx.
5. RMS Noise:	
0.1 gauss range	25 db below full scale approx.
0.3 gauss range	35 db below full scale approx.
1 g to 30 kG range	45 db below full scale approx.

(g) Power Requirements:

1. Line input:

Volts	105-125 V or	210-250 V
Frequency	50-60 Hz	50-60 Hz
Current	0.038 A	0.019 A
Power	4 W	4 W

2. Battery input:
9 V to 18 V at approx. 130 mA, automatic take over in case of failure in line voltage

3. Internal battery:
12 V dry battery, Neda 923—Eveready 2780N; automatic take over in case of failure in line voltage (approx. 100 h life with continuous use)

to check the internal battery condition or external dc input voltage.

4. Probe Zero Controls:
COARSE and FINE zeroing controls are provided to balance each individual probe for zero output in the absence of a magnetic field. They will also suppress small residual fields up to approximately 30 gauss. By turning the FINE control full CCW past the switch, the zero controls can be disconnected, permitting the instrument to be used with special probes having their own zero controls.

5. CAL FS Control:
The screwdriver CAL control is used to calibrate the instrument using the internal calibration feature as well as calibration to a standard magnet. Calibration through external indicating instruments is also possible with connection to the output jacks.

GAUSSMETER PROBES

THIRD GENERATION

Look AT Cable End of Probe For Number

HTB4 -0608
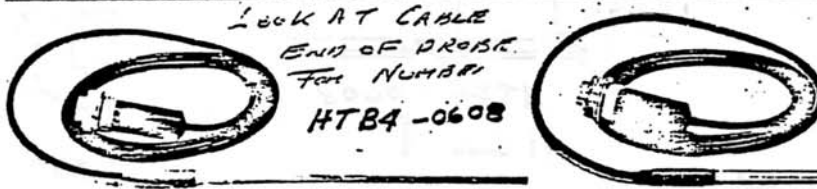
DESCRIPTION

The third generation of Bell gaussmeter probes is comprised of a wide range of probe models designed to meet the electrical and mechanical requirements of virtually any application. The probes are precision, solid state magnetic field sensors built for accurate, repeatable, stable field measurements. Models are available for transverse, axial, two axis, or three axis field measurements with a variety of field measurements ranges, field sensitivities and physical configurations for each. Calibrated extension cables and high sensitivity magnaprobes are also available.

The third generation supercedes and replaces all other Bell gaussmeter probes. The lower price, improved quality, and increased model selection are the benefits of new technology and experience. Individual probe linearity curves are available as an option. CAUTION! Probes are fragile! Handle with care!

MODEL NUMBERING

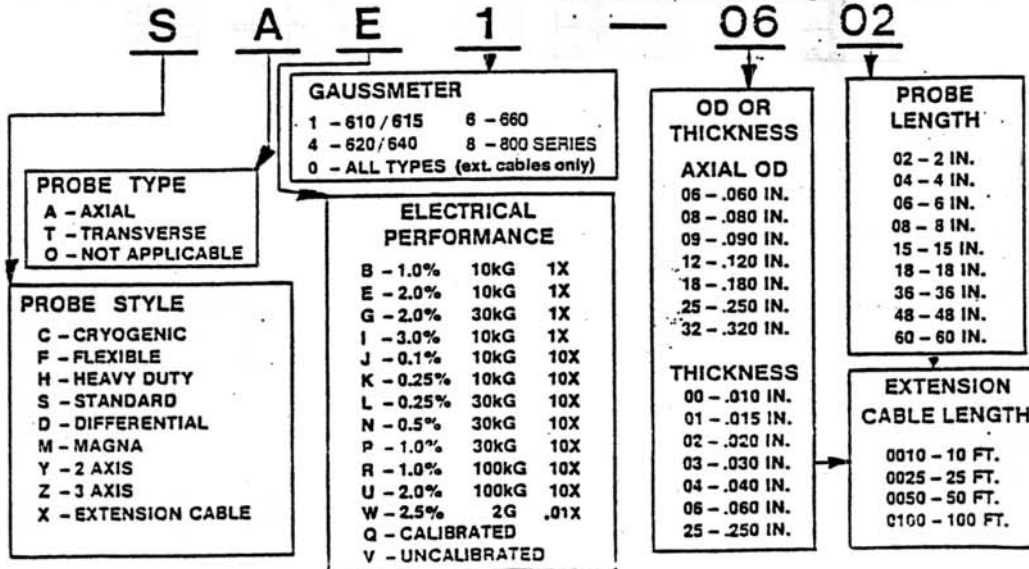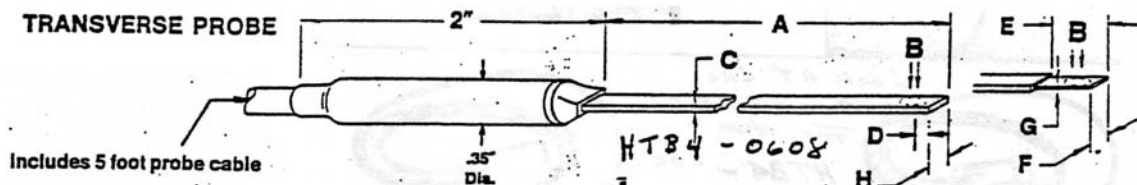Each probe model is classified with a three letter, five numeral model number. The chart below shows the significance of each letter and numeral. At the factory the assembled probes are calibrated to match the input characteristics of each gaussmeter model. The model to which the probe is calibrated is indicated by a numeral in the fourth space of the model number. A model SAE1-0602 will operate properly with any model 610 gaussmeter. The model SAE6-0602 will only work with a model 660 gaussmeter although it is physically identical to the SAE1-0602. With their proper respective gaussmeters the probe model SAE1-0602 and model SAE6-0602 have the same characteristics. Thus, to simplify the model listing the fourth space has been omitted. Please insert the number which corresponds to the gaussmeter that will be used with the probe. The sensitivity number is the constant by which the meter reading is multiplied to obtain the actual reading.

S A E 1 — 06 02

GAUSSMETER

1 – 610 / 615	6 – 660
4 – 620 / 640	8 – 800 SERIES
0 – ALL TYPES (ext. cables only)	

PROBE TYPE

A – AXIAL
T – TRANSVERSE
O – NOT APPLICABLE

PROBE STYLE

C – CRYOGENIC
F – FLEXIBLE
H – HEAVY DUTY
S – STANDARD
D – DIFFERENTIAL
M – MAGNA
Y – 2 AXIS
Z – 3 AXIS
X – EXTENSION CABLE

ELECTRICAL PERFORMANCE

B – 1.0%	10kG	1X
E – 2.0%	10kG	1X
G – 2.0%	30kG	1X
I – 3.0%	10kG	1X
J – 0.1%	10kG	10X
K – 0.25%	10kG	10X
L – 0.25%	30kG	10X
N – 0.5%	30kG	10X
P – 1.0%	30kG	10X
R – 1.0%	100kG	10X
U – 2.0%	100kG	10X
W – 2.5%	2G	.01X
Q – CALIBRATED		
V – UNCALIBRATED		

OD OR THICKNESS

AXIAL OD

06 – .060 IN.
08 – .080 IN.
09 – .090 IN.
12 – .120 IN.
18 – .180 IN.
25 – .250 IN.
32 – .320 IN.

THICKNESS

00 – .010 IN.
01 – .015 IN.
02 – .020 IN.
03 – .030 IN.
04 – .040 IN.
06 – .060 IN.
25 – .250 IN.

PROBE LENGTH

02 – 2 IN.
04 – 4 IN.
06 – 6 IN.
08 – 8 IN.
15 – 15 IN.
18 – 18 IN.
36 – 36 IN.
48 – 48 IN.
60 – 60 IN.

EXTENSION CABLE LENGTH

0010 – 10 FT.
0025 – 25 FT.
0050 – 50 FT.
0100 – 100 FT.

TRANSVERSE PROBE

Includes 5 foot probe cable · .35 Dia. · HT84-0608

| Model	Price	A	H	C		E	F	G	Stem Material			Active Area	Operating Temperature Range	Temperature Stability (max.) Zero	Calibrate
STB— -0402	5118	2"±.063								1% to 10 kG	1x blue	.070" dia. nom.		±.09 Gauss /°C	—.04 %/°C
STB— -0404	124	4"±.063								2% to 30 kG					
STG— -0402	141	2"±.063	.150" ±.004	.040" +.000 -.004		Not Applicable	Not Applicable	Not Applicable	Rigid Glass Epoxy	.1% to 10 kG	10x red	.040" dia. nom.	0°C to +75°C	±.13 Gauss /°C	±.005 %/°C
STG— -0404	148	4"±.063								.25% to 30 kG					
STJ— -0402	218	2"±.063								1% to 100 kG					
STJ— -0404	224	2"±.063													
STL— -0402	277	4"±.063													
STL— -0404	282	4"±.063													
STR— -0402	336	2"±.063													
STR— -0404	341	4"±.063													
HTB— -0608	129	8"±.125								1% to 10 kG	1x blue	.070" dia. nom.		±.09 Gauss /°C	—.04 %/°C
HTB— -0618	141	18"±.125								2% to 30 kG					
HTG— -0608	153	8"±.125	.180" ±.003	.060" +.000 -.004	.145" ±.063				Aluminum	.1% to 10 kG	10x red	.040" dia. nom.		±.13 Gauss /°C	±.005 %/°C
HTG— -0618	165	18"±.125								.25% to 30 kG					
HTJ— -0608	230	8"±.125								1% to 100 kG					
HTJ— -0618	242	18"±.125													
HTL— -0608	289	8"±.125													
HTL— -0618	301	18"±.125													
HTR— -0608	348	8"±.125													
HTR— -0618	360	18"±.125													
CTP— -3248	589	48"±.25	.312" ±.005 dia.	Not Appli-cable	.320" ±.063				Stainless Steel	1% to 30 kG			—269°C to +75°C		±.01 %/°C
CTP— -3260	589	60"±.5								2% to 100 kG					
CTU— -3248	647	48"±.25													
CTU— -3260	647	60"±.5													
STB— -0204	129									1% to 10 kG	1x blue	.070" dia. nom.	0°C to +75°C	±.09 Gauss/°C	—.04 %/°C
STG— -0204	153									2% to 30 kG					
STJ— -0204	230	4" ±.063	.155" ±.005			.130" ±.008	.375" ±.063	.130" ±.003	.020" ±.003	Semi-rigid	.1% to 10 kG	10x red	.040 dia. nom.		±.13 Gauss/°C	±.005 %/°C
STL— -0204	289									.25 % to 30 kG					
STR— -0204	348									1% to 100 kG					
STE— -0104	301					.055" ±.005	.312" ±.031	.080" ±.003	.015" +.000—.003		2% to 10 kG	1x blue			±.15 Gauss/°C	—.08%/°C
STI— -0004	454					.050" ±.005	.375" ±.063	.135" ±.005	.010" +.000—.003		3% to 10 kG	1x blue	.030" dia. nom.	0°C to +50°C	±.20 Gauss/°C	—.10%/°C

15

APPENDIX VI

THE RESONANCE ISOLATOR
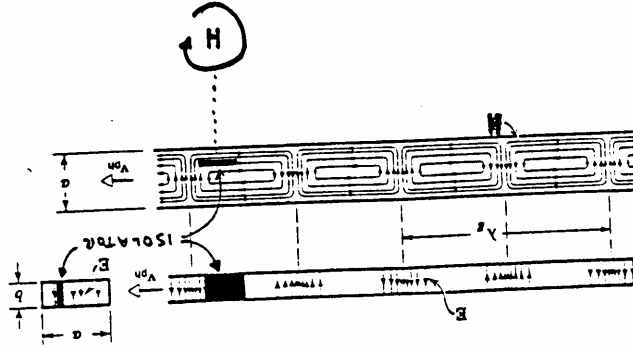
Figure VI-1: Wave Guide Cross Sections Showing the Position of the Ferrite Slab.

The explanation of absorption in the resonance isolator is quite similar to the explanation for absorption in the cavity.

The isolator consists of a ferrite slab with step shaped pieces of dielectric at the ends for matching purposes. The ferrite slab sits in a field of 0.2 to 0.3 tesla produced by a permanent magnet and the electrons in the ferrite precess at microwave frequencies.

It can be seen from figure VI-1, that at the position of the ferrite slab, the magnetic field due to the microwaves rotates with uniform amplitude. If the sense and frequency of rotation of the magnetic field is the same as the precession of the electrons in the field of the permanent magnet, then absorption of the microwaves will result. For microwaves travelling in the opposite direction, the rotation of the microwave magnetic field at the position of the ferrite slab is in the opposite sense and no absorption will take place.

The magnetic field due to the permanent magnet is normal to the paper and it is left to the student to determine the exact direction so that microwaves travelling to the right will be transmitted while those travelling to the left will be absorbed. Conclusions should be checked empirically since one knows from the apparatus the direction of the permanent magnetic field and the direction of travel for the transmitted waves.